SOILS AND FOUNDATIONS Vol. 36, No. 2, 81-91, June 1996
Japanese Geotechnical Society

THE STEADY STATE OF SANDY SOILS

RAMON VERDUGO[i] and KENJI ISHIHARA[ii]

ABSTRACT

An alternative procedure to evaluate the void ratio of triaxial test samples is introduced. This method is recommended particularly when very loose samples are tested and an important volume change occurring during the saturation process is expected. In addition, using Toyoura sand a comprehensive set of triaxial tests carried out under both undrained and drained conditions of monotonic loading is presented. For the undrained contractive responses, the results showed two stages associated with the steady state. After the peak strength, the deviator stress drops to a minimum value which can be seen as a quasi steady state, thereafter, the strength increases to an ultimate value corresponding to the actual steady state. Undrained dilative responses clearly indicated the existence of an ultimate state developed at large deformations which represents the steady state of deformation. The results indicate that the quasi steady state is slightly affected by the initial mean stress, whereas, the steady state is unaffected by the initial mean stress. Furthermore, the locus of the ultimate states achieved through drained conditions of loading was shown to be coincident with the steady state line evaluated by means of undrained tests. Finally, according to the relative position of the steady state line with respect to the isotropic consolidation curves for the loosest and densest states of a given soil, the index, Relative Contractiveness, R_c, is proposed. It is postulated that R_c is related to the inherent liquefaction vulnerability of a soil.

Key words: liquefaction, sandy soil, silt, triaxial compression test, undrained shear (**IGC**: D6/D7)

INTRODUCTION

In the past, the term "liquefaction" has been used to describe all phenomena that are related with the undrained response of cohesionless material where an important build up of pore water pressure as well as a significant amount of deformation take place. At least two different phenomena, however, should be distinguished: flow failure or true liquefaction and cyclic mobility. Although these concepts were presented early by Casagrande (1975) and Castro (1975), perhaps only since the last decade they have been widely recognized and accepted. The phenomenon defined as "true liquefaction" is characterized by a quick increment of pore water pressure followed by a sudden loss of strength until a residual value is achieved. The term "cyclic mobility" introduced by Casagrande (1975) denotes the undrained cyclic soil response where the soil mass does not undergo any loss of strength, but it undergoes a kind of strain softening, which is mainly a consequence of the build up of pore water pressure caused by the cyclic loading. The study discussed herein is concerned with the first phenomenon.

Recently, interest in the importance of developing a suitable methodology to analyze the stability of saturated poorly compacted sandy soil deposit has increased. This fact comes as a consequence of the occurrence of large landslides in natural slopes, dam failures and flow failures of hydraulic placement of artificial island fills or reclaimed land areas along coast lines (Ishihara et al., 1991). A better understanding and a more suitable characterization of the undrained response of saturated cohesionless materials are therefore needed. Consequently, in the present study experimental evidence useful to obtain a better understanding of sandy soil behavior is presented. In addition, a parameter to identify the intrinsic potential for liquefaction of a given soil is introduced.

TESTING EQUIPMENT AND SOIL TESTED

In order to cover a wide range of confining pressures, and at the same time to have accurate measurements, two triaxial test apparatuses designed for a different level of pressure and load were used. A low and a high pressure triaxial cell for maximum pressures of 1 MPa and 5 MPa were designed. For each test, the most appropriate test apparatus was selected depending on the desired confining pressure and the anticipated undrained response. For instance, when large dilative behavior of the soil specimen

[i] Geotechnical Section IDIEM University of Chile, Plaza Ercilla 883, Santiago, Chile. Former Graduate Student, Univ. of Tokyo, Japan.
[ii] Former Professor, Department of Civil Engineering, University of Tokyo, Bunkyo-ku 113, Tokyo.
Manuscript was received for review on May 17, 1994.
Written discussions on this paper should be submitted before January 1, 1997 to the Japanese Geotechnical Society, Sugayama Bldg. 4 F, Kanda Awaji-cho 2-23, Chiyoda-ku, Tokyo 101, Japan. Upon request the closing date may be extended one month.

was expected, the cavitation was effectively avoided by means of high back pressure using the high pressure apparatus. Lubricated as well as enlarged end plates were used in order to minimize non-homogeneities in the strain distribution throughout the samples and particularly to avoid the development of shear bands. The axial load, pore water pressure, axial deformation and volumetric strain were measured by electrical transducers and automatically stored in a personal computer. All the tests were conducted under strain-controlled condition of loading. The deformation rates were 1 and 0.5 mm/min for undrained and drained tests, respectively. The initial dimensions of the specimens were 5 cm in diameter and 10 cm in height for those specimens tested in the low pressure triaxial cell, and 6 cm in diameter and 12 cm in height in the case of samples tested in the high pressure cell.

All the tests were performed on the standard Japanese Toyoura sand. This sand has a mean diameter of $D_{50}=0.17$ mm, a uniformity coefficient of $U_c=1.7$, a maximum void ratio of 0.977, a minimum void ratio of 0.597, and a specific gravity of 2.65. Toyoura sand is a uniform fine sand consisting of subrounded to subangular particles and composed of 75% quartz, 22% feldspar and 3% magnetite (Oda et al., 1978).

SAMPLE PREPARATION

To prepare the specimens, the so-called moist placement or wet tamping method of sample preparation was used. Oven dry soil was mixed well with distilled water in a proportion of 5% by weight and compacted in six and ten layers in the case of the low and high pressure apparatus, respectively. After the initial density was determined, and the total weight computed, each layer was carefully compacted with identical height and amount of wet soil. Thereafter, the specimens were installed in the pedestal and CO_2 gas followed by de-aired water circulated throughout from the bottom to the top. After the cell was assembled, the degree of saturation was improved by means of back pressure which was considered acceptable when the B-value was equal to or greater than 0.95.

EVALUATION OF SAMPLE VOID RATIO

Samples loosely compacted are susceptible to potential error in the evaluation of the void ratio. During the saturation process a partial collapse of the unstable structure occurs and a significant variation in the sample dimension takes place, which can not be measured using ordinary test procedures (Sladen et al., 1987). Two alternative procedures to assess the void ratio of the specimens after they have been saturated were therefore developed which are described below:

a) Using sample dimensions.—This method corresponds to the ordinary procedure based on the direct evaluation of the height and diameter of the samples after CO_2 and de-aired water have been percolated throughout the specimens, and therefore, any possible collapse has occurred. An improvement in the procedure has been used however, avoiding the dismanteling of the cell after the saturation of the samples has been completed. After the air in the voids of the sample has been replaced by CO_2, a vacuum of 0.02 MPa for the sample tested in the low pressure triaxial cell and 0.05 MPa for the sample tested in the high pressure triaxial cell was applied through the upper and lower drainage lines of the specimen with tanks A and B as illustrated in Fig. 1(a). When the vacuum is applied, the position of tanks A and B is such that the water level in the tanks is below the sample. Next, in order to induce percolation of water throughout the specimen under vacuum, tank A is moved up from its initial position to a second location approximately 50 cm above the top of the sample. As the water flows into the specimen, a sort of collapse on the very loose soil structure occurs, and accordingly, the sample dimensions change. The percolation of water is performed until in the pipe connected to the top of the sample air bubbles are not observed any more. Thereafter, tank A is moved down to its initial position and then the dimensions of the sample are measured. The diameters were taken to an accuracy of 0.01 cm with a calibrated metal tape and the height was measured to an accuracy of 0.01 cm by means of a calibrated caliper. Consequently, the initial volume of the sample was evaluated and modified later considering the volume change that occurs during consolidation.

b) Using the water content of the specimen.—This method was developed considering that for saturated samples, the void ratio is directly related with the amount of water in the sample. For clayey soils, the procedure

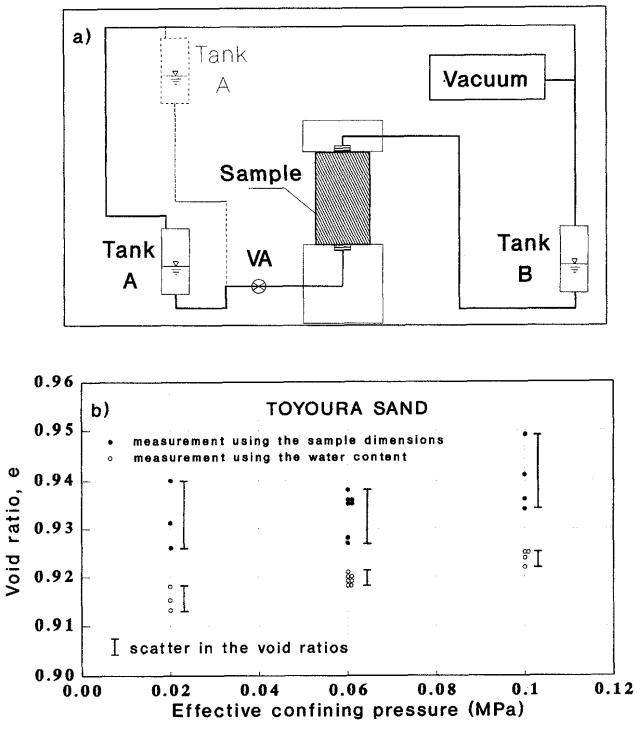

Fig. 1. a) System for water circulation; b) Comparison between water content and sample dimension procedures for evaluation of sample void ratio

does not involve significant difficulty, but in sandy soils some special technique is necessary, for instance, "freezing" the sample. The authors have developed an alternative method however that seems to be simpler than the current procedures, which involve the following steps: after the test is finished, the drainage valves are closed, so that the specimen is in an undrained condition. The back pressure on the lines is completely released and the level of the water in the burette, V_i, is recorded. The drainage valves are then opened and connected to the burette. Next, the cell pressure is increased to the maximum capacity of the equipment, and then an axial loading and unloading process is applied in order to remove from the sample as much water as possible which flows into the burette. Thereafter, the cell pressure is decreased to around 0.2 MPa, the drainage valves are closed again, and the level of the water in the burette, V_f, recorded. Then, the cell pressure is totally released and the triaxial cell dismounted. Because the specimen is finally unloaded under an undrained condition, it develops a negative pore water pressure which allows the sample to remain upright. Next, the upper cap is removed and air goes into the sample (because of the negative pore water pressure) creating an apparent cohesion that permits the sample to be handled. Immediately, the membrane is removed from the sample, and by means of a spatula, all the soil attached to both the membrane and to the end platens is carefully removed. The remaining water content of the soil sample, ω_r, is then measured. Therefore, the void ratio of the specimen can be computed from the following expression:

$$e=\frac{(V_f-V_i+\omega_r W_d)}{W_d} G_s \qquad (1)$$

where, W_d is the dry weight of the sample and G_s is the specific gravity of the soil.

The first method is basically the common practice to evaluate the void ratio of a sample, while the second method is an alternative procedure. To investigate the effectiveness of this alternative procedure, three series of samples were prepared repeating as close as possible all the steps involved in the preparation. Figure 1(b) shows the results of these three series of tests. It can be observed that the scattering in the void ratios evaluated through the water content is much smaller than the one obtained by the ordinary procedure using the sample dimensions. This fact is indicative of the repetitiveness and effectiveness of the proposed procedure. In addition, as shown in Fig. 1(b), the results using these two procedures consistently indicated that the void ratios measured through the water content were smaller than the void ratios computed from the sample dimensions. For dense specimens however, the difference between these two methods was negligible. The discrepancy between these two methods may arise from the subsequent steps wherein the triaxial cell is assembled and likely, some additional volume change takes place which can not be computed by the first method. The procedure based on the measurement of the water content at the end of the test has therefore been adopted as a more reliable procedure to evaluate the void ratio. Hence, void ratios estimated by this method have been used as the representative values of the samples and reported in this paper.

MONOTONIC UNDRAINED RESPONSE

Three series of undrained monotonic compression tests with consolidation pressures varying in a wide range and constant void ratios achieved after consolidation, were carried out. Figure 2 for example, shows the stress-strain curves and the corresponding effective stress paths for a series of tests with a common void ratio after consolidation of $e=0.735$. The effective mean stress is evaluated as $p'=(\sigma_1+2\sigma_3)/3$ and the deviator stress as $q=(\sigma_1-\sigma_3)$. As can be seen, the soil response is such that an ultimate condition is developed at large deformation which is identical to all the specimens, independent of the initial confining pressure. It is important to note that during unloading the effective stress paths are coincident, suggesting that a special common fabric was developed at large deformation.

Another series of tests performed with a void ratio after consolidation of $e=0.833$ and different initial confining pressures is shown in Fig. 3 in terms of stress-strain curves and effective stress paths. For initial confining pressures of 2 and 3 MPa, the response of the specimens shows a drop in strength, and consequently, the specimens develop a minimum strength which occurs between 5 to 10% of axial strain. It is of interest to note, that the minimum strength developed is

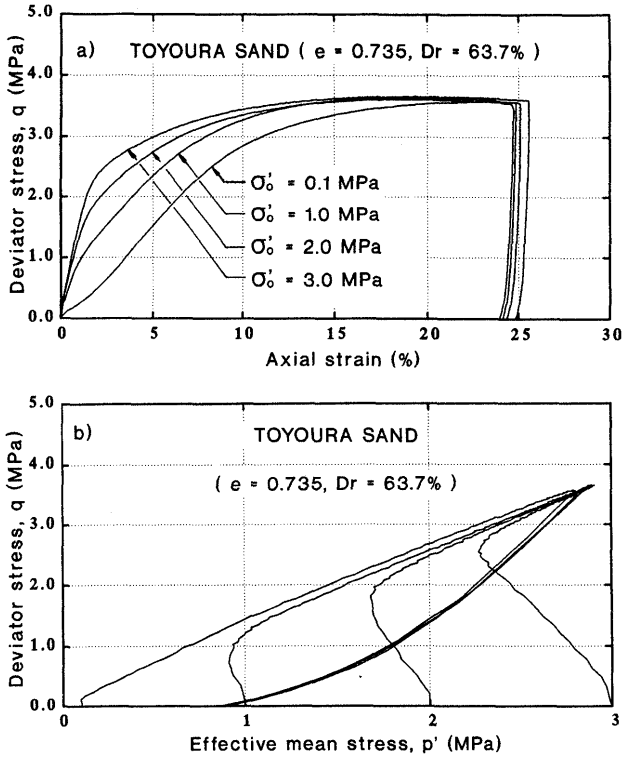

Fig. 2. Undrained triaxial tests for $e=0.735$: a) stress-strain curves; b) effective stress path

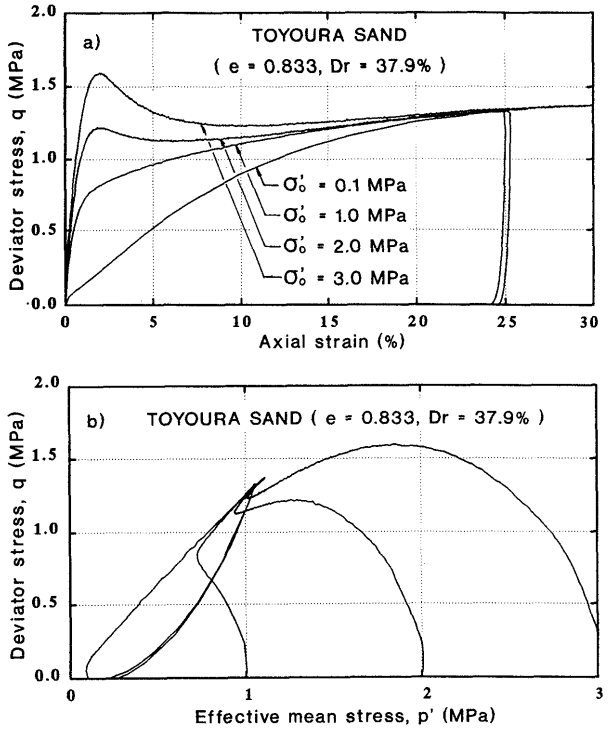

Fig. 3. Undrained triaxial tests for $e=0.833$: a) stress-strain curves; b) effective stress path

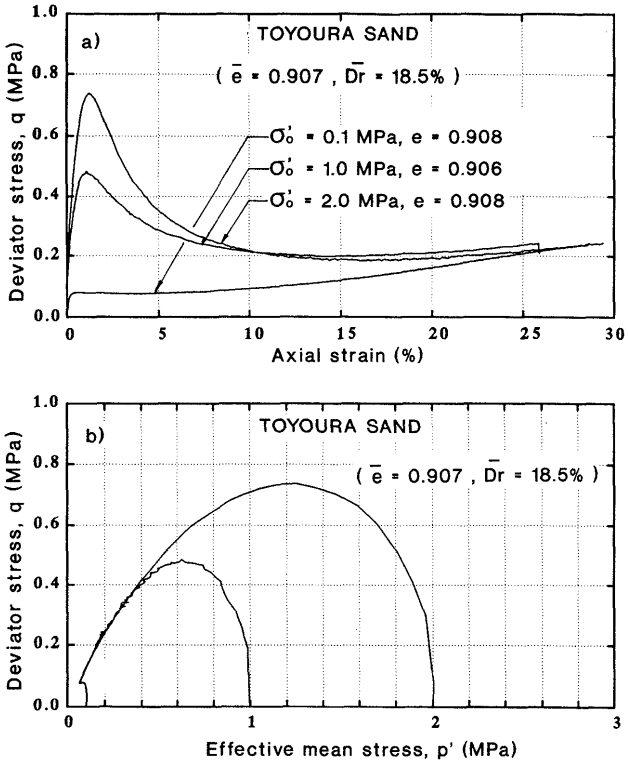

Fig. 4. Undrained triaxial tests for $e=0.907$: a) stress-strain curves; b) effective stress path

slightly affected by the initial effective confining pressure. It should also be noted that, despite the large difference in the stress-strain behavior at an early stage of the loading, the samples tend to have the same ultimate strength at a large level of deformation. In addition, in this series, the effective stress paths during unloading are coincident with each other suggesting the development of a common fabric at the stage of large deformation. The stress-strain curves and the corresponding effective stress paths for another series of tests performed with a void ratio after consolidation of $e=0.906$–0.908 and with effective confining pressures varying from 0.1 to 2 MPa are shown in Fig. 4. As can be observed, for the complete range of pressure used, the soil behavior indicates a peak deviator stress, and the higher the initial confining pressure the higher the peak deviator stress. A minimum strength is developed at a medium range of axial deformation between 4 to 16%. As the previous results, the minimum strength seems to be only slightly affected by the initial confining pressure, while the ultimate deviator stress developed in these three specimens is the same, regardless of the value of the initial confining pressure. It is also of interest to note that for the specimen consolidated under 0.1 MPa, the effective stress path reaches the ultimate state to the right of the initial state indicating that, the response is finally dilative, even though in the range of axial deformation between 1 to 6%, the behavior was clearly contractive with a small drop of strength. It is important to mention that, in this case, the condition of continuous deformation under a constant shear stress level is not strictly satisfied at large deformation. The rate of variation nevertheless is rather small, so in this situation the state of stress developed close to 26% of axial strain has been considered as the condition associated with the ultimate state. The authors believe that the stresses developed at this level of deformation are from any practical point of view, close enough to the actual ultimate condition in the case of sandy soils.

This series of undrained test results have shown two soil responses, a dilative one with a deviator stress that is always monotonically increasing up to an ultimate state achieved at large deformation where the soil sample deforms continuously under a constant shear stress, and constant effective mean stress. Another soil response is the contractive one with the development of a minimum strength that is followed by a dilative behavior where the strength is regained and it eventually reaches an ultimate value at large strains. The latter soil response indicates two particular conditions that require especial attention: a) the minimum strength and b) the ultimate state developed at large strain level. These stages are of particular importance due to the fact that they represent different levels of strength. It is apparent that these two conditions can be associated with the steady state of deformation (Poulos, 1981), because the requirements of continuous deformation under constant shear stress and constant normal stress are to some extent satisfied. The additional requirement of constant volume is automatically satisfied during undrained tests and the condition of constant velocity is fully satisfied by the strain controlled loading system.

The condition of minimum strength has been referred

to as the quasi steady state, (Alarcon-Guzman et al., 1988; Ishihara, 1993; Verdugo, 1992) whereas, the condition reached at large level of strain is likely associated with the actual steady state. The shear stress mobilized at the minimum strength stage is definitely smaller than the stress mobilized at the ultimate steady state, however, the strain level required for the ultimate state is much larger than the strain associated with the minimum strength.

THE QUASI STEADY STATE

From those specimens where a drop in strength takes place, the minimum strength condition or the quasi steady state has been plotted in Fig. 5 in terms of void ratio and effective mean stress. The initial states of void ratio and consolidation pressures are indicated by squares. As can be observed, for the wide range of initial effective confining pressures and void ratios used, there exists a clear correlation between the void ratio and the effective mean stress developed at the stage where the minimum strength is mobilized. This line is referred to as the quasi steady state line (Verdugo, 1992; Ishihara, 1993). In spite of the clear trend shown in Fig. 5 by the quasi steady state line, some scatter in the data is apparent. This is due to the fact that the mobilized minimum strength is affected to some degree by the initial consolidation pressure. The larger the initial effective confining pressure, the larger the minimum strength and the corresponding effective mean stress. Nevertheless, the experimental results indicate that this effect is not significant and accordingly, it would be possible to draw a single line representing an average condition of the quasi steady state in the e-p' plane and use it as a convenient reference line to facilitate the evaluation of the minimum strength. It has been shown elsewhere (Verdugo, 1992; Ishihara, 1993) however, that this line is strongly affected by both the initial fabric and structure of a soil mass. The use of the quasi steady state line is therefore restricted to those cases where the soil deposit and the soil sample tested in the laboratory have similar fabric.

The contractive response is only developed by those samples with an initial combination of void ratio and effective mean stress that can be represented by a point located well above the steady state line in the e-p' plane. This observation confirms previous results reported by Castro (1969); Castro et al. (1982); Been et al. 1985; Dobry et al. (1985), and Poulos et al. (1985), among others.

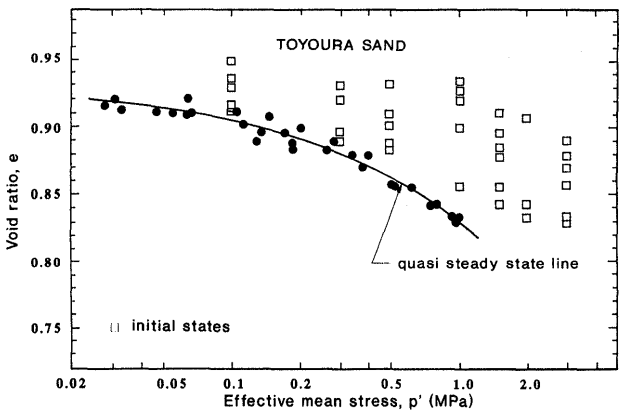

Fig. 5. Quasi steady state line and initial states

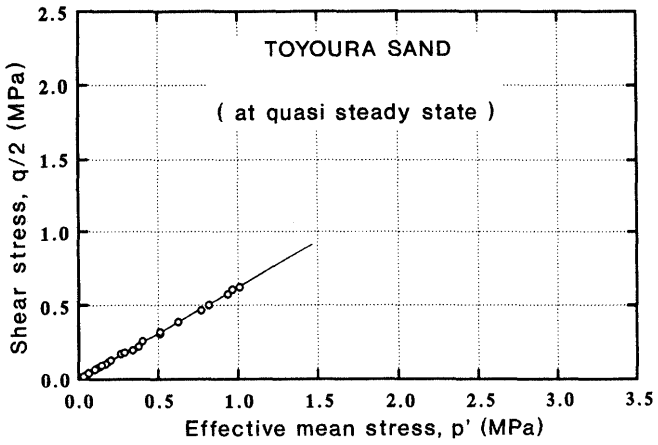

Fig. 6. Strength envelope at the quasi steady state

It is of particular importance to mention that the state of minimum strength coincides with the condition of phase transformation introduced by Ishihara et al. (1975). The phase transformation was defined however to imply a temporary state of transition from contractive to dilative behavior of sand, irrespective of whether it involves a temporary drop in shear stress or not. The quasi steady state has to be seen therefore as the particular case of phase transformation where a temporary drop in shear stress takes place over a limited range of shear strains.

Regarding the resistance developed during the quasi steady state, it can be easily understood that the shear stress mobilized at this stage of deformation is a consequence of frictional resistance between the particles of the soil. The effective normal stress and shear stress should therefore be uniquely correlated through some angle of internal friction. To explore this aspect, the shear stress, $q/2$, and the effective mean stress, p', attained at the quasi steady state have been plotted in Fig. 6. As can be observed, the state of stresses at the quasi steady state can be represented fairly well by a straight line passing through the origin in the $q/2$-p' plane. The angle of internal friction obtained from these data is close to 31°.

THE STEADY STATE OR ULTIMATE STATE FROM UNDRAINED TESTS

Under undrained loading condition, irrespective of the initial state of the specimens, when the strain level is large enough, the soil mass tends to be in a state of continuous deformation under constant shear stress and constant mean stress. This stage of the soil response is quite apparent in those tests shown in Figs. 2 and 3 when the axial strains are larger than 20–25%. As can be observed in Fig. 4 however, there are responses where the deviator stress and the effective mean stress are still increasing af-

ter an axial strain of 28%. Nevertheless, the increments are small and always at a decreasing rate, hence in these cases, the stresses at an axial strain around 26% have been taken as representative of the ultimate state of the specimens. In Fig. 7, a good correlation can be observed between the specimen void ratios and the effective mean stress developed at large deformation, which corresponds to the steady state line. The initial states of the samples are indicated in Fig. 7 by squares showing that, in contrast to the quasi steady state line, the steady state line can be obtained independently of the initial state of the specimens. In addition, experimental results reported by Verdugo (1992) and Ishihara (1993) have shown that the steady state line is unaffected by the initial fabric as long as the soil mass is homogeneous.

Concerning the frictional resistance developed at this state, Fig. 8 shows the shear stress, $q/2$, and the effective mean stress, p', computed from each test. As can be seen, all the data points fall in a straight line passing through the origin indicating that a unique friction angle is mobilized at the ultimate state or steady state which is in perfect agreement with experimental data reported by Negussey et al. (1988) using ring shear tests. For Toyoura sand, the experimental results indicated that the slope of this line is close to 0.62, confirming a friction angle in the steady state of deformation of around 31°.

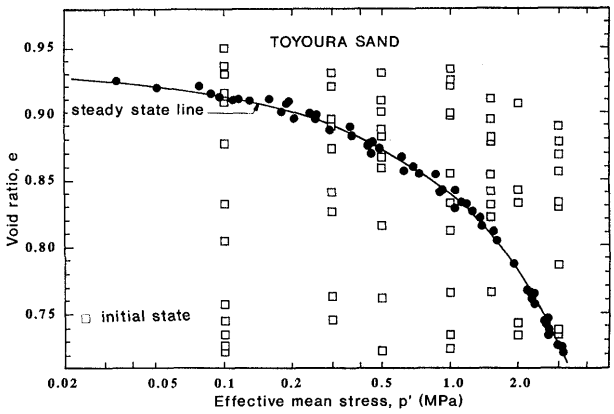

Fig. 7. Steady state line and initial states

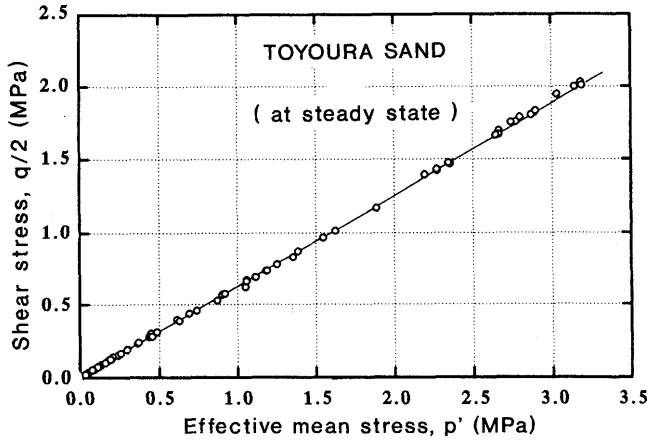

Fig. 8. Strength envelope at the steady state

MONOTONIC DRAINED RESPONSE

A series of conventional triaxial tests with constant lateral stress under drained condition of loading were performed for three different states of packing; very loose, loose and medium. The deviator stress versus axial strain and void ratio for consolidation pressures of 0.1 and 0.5 MPa, are shown in Figs. 9 and 10, respectively. As can be observed, under a small level of strain, the stress-strain curves are different depending upon the initial density of the sample. As the level of strain becomes large however, all the curves merge into a single one. Similar behavior is observed in terms of deviator stress and void ratio. Initially, at zero level of shear stress, the starting void ratios are different, but as the strain level increases, the curves tend to achieve a common void ratio and a common deviator stress, which confirms experimental results reported by Casagrande (1936), Roscoe et al. (1958) and Been et al. (1991). The soil response achieved at a large level of strain under drained condition of loading therefore can be seen as the corresponding drained steady state of deformation

For all the tests performed under drained condition of loading, Fig. 11 shows the paths in terms of void ratio and mean stress. The circles indicate the data points related to the steady state condition evaluated from undrained tests, and the black squares indicate the ultimate

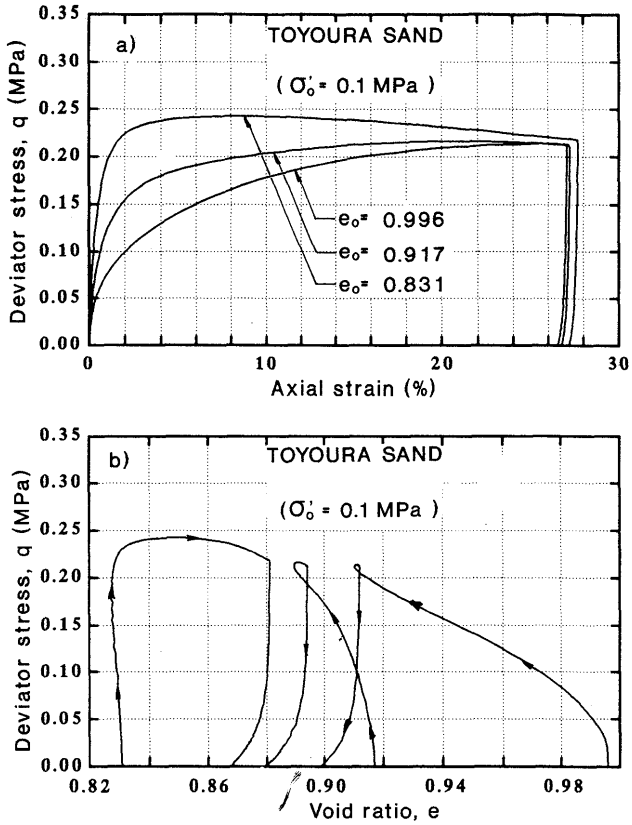

Fig. 9. Drained triaxial tests for σ'_0=0.1 MPa: a) stress-strain curves; b) void ratio versus deviator stress

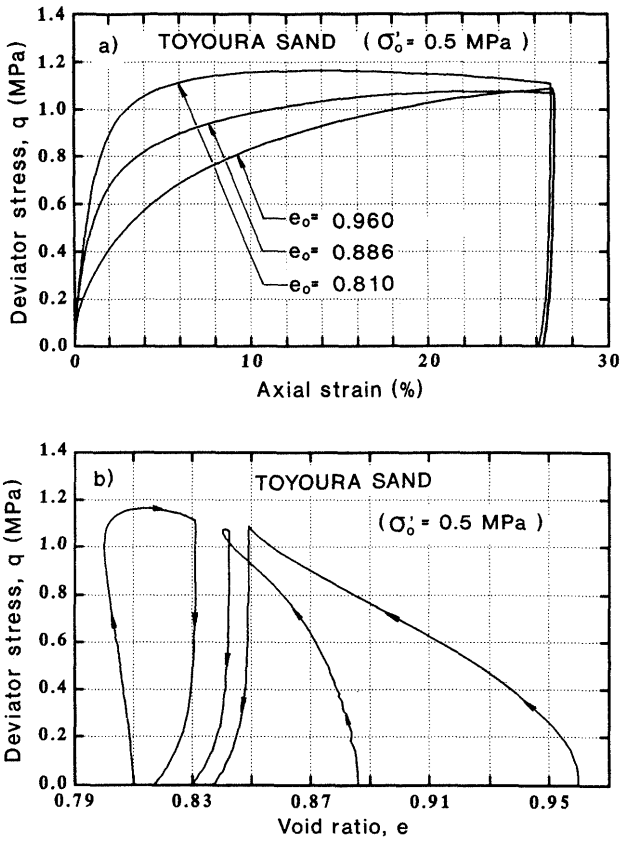

Fig. 10. Drained triaxial tests for σ_0'=0.5 MPa: a) stress-strain curves; b) void ratio versus deviator stress

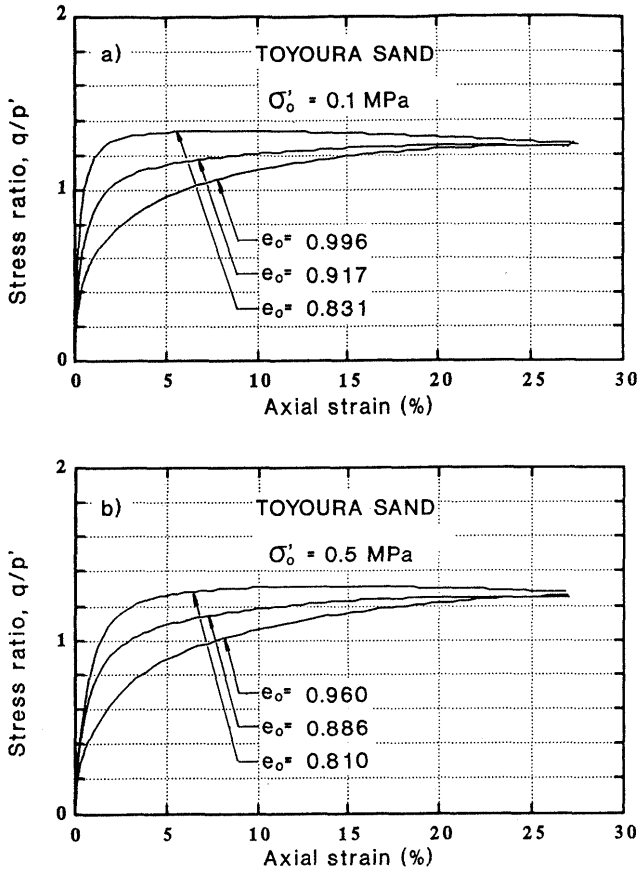

Fig. 12. Stress ratio, q/p', versus axial strain for a) σ_0'=0.1 MPa and b) σ_0'=0.5 MPa

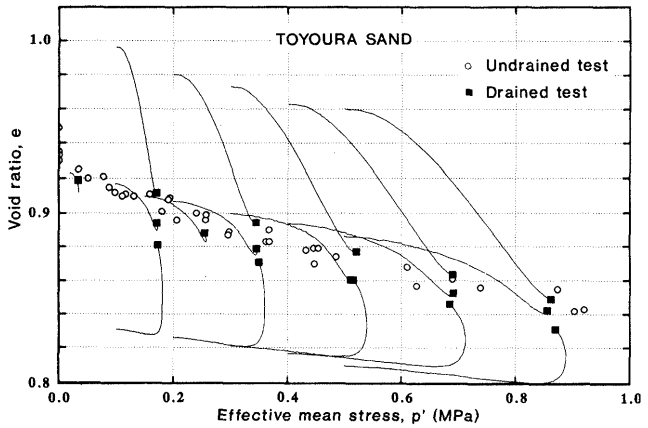

Fig. 11. State diagram evaluated from both drained and undrained triaxial tests

conditions achieved by the drained tests which should be associated with the drained steady state. As can be observed, there is a very good agreement between the steady state conditions obtained from both undrained and drained tests. It is important, however, to note that even though the general trend presented by the drained tests is clear, the scatter in the data points concerning the ultimate state of these tests is much more significant than those obtained for the case of undrained tests. In this regard, it seems that drained tests are not the most suitable tests to evaluate the steady state line with undrained tests being more preferable.

In addition, for three different initial densities and for consolidation pressures of 0.1 and 0.5 MPa, the stress ratio, q/p', versus the axial strain are shown in Figs. 12(a) and (b), respectively. It can be seen that at a large strain level, the mobilized stress ratio, q/p', is constant and independent of the initial density and confining pressure. This fact indicates that, for the level of pressures and densities investigated, the friction angle mobilized at a large strain level is unique and unaffected by sample density and consolidation pressure. In addition, the computed value of $q/2p'$ is close to 0.62 which is about the same value obtained from undrained tests. The friction angle mobilized at the steady state condition therefore is a unique value regardless of the density, level of pressure, and type of loading (drained or undrained).

CHARACTERISTIC LINES IN THE *e-p'* PLANE

The *e-p'* plane provides a good representation of the steady state line, and it may also be useful to define boundaries which can characterize the soil response. For sandy and silty soils it is conceptually possible to define an upper boundary using the isotropic consolidation curve for the loosest state that a given cohesionless soil may attain. This curve is equivalent to the normal consoli-

dated curve for clays in the sense that defines a limit over which a combination of void ratio and effective mean stress can not exist. It is important, however, to keep in mind that this curve may be different for different sample preparation procedures as shown in Fig. 13 (Ishihara, 1993). It is recommended that the consolidation curve for the loosest state be evaluated by means of a sample performed by the moist placement (wet tamping) method of preparation and then saturated. Based on the authors' experience, this method of sample preparation permits the achievement of the loosest packing compared to any other method of sample preparation. In some soils it even provides a larger void ratio than the maximum void ratio evaluated using either the USA or the Japanese codes (Verdugo, 1992).

Similar to the upper boundary defined by the consolidation line of the loosest state, it is possible to define a lower boundary. For the common range of pressures anticipated in engineering practice, the isotropic consolidation curve for the densest packing provides the lowest limit of states in the *e-p'* plane. For Toyoura sand both the isotropic consolidation curve for the loosest and densest state are shown in Fig. 13 (Ishihara, 1993). It is readily apparent that for the case of the densest state, the volumetric strains caused by isotropic loading are very small even though the confining pressure is significantly high. For practical purposes therefore this curve can be approximated by a horizontal straight line passing through the minimum void ratio. This simplification is obviously limited by the pressure from which the particle crushing began to be important. According to the test results shown in Fig. 13, in the case of Toyoura sand this pressure would be greater than 4 MPa which includes most of the cases encoutered in practice. There are other soils such as carbonate containing sands and decomposed granite sandy soils however that are much more crushable. For these soil types the proposed simplification is still valid, but for a smaller region. Nevertheless, if the particular soil under consideration seems to be extremely crushable, the simplification can be avoided and the corresponding isotropic consolidation test for the densest state performed.

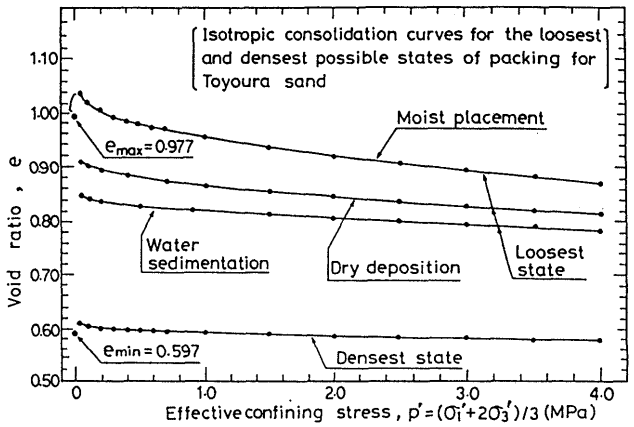

Fig. 13. Isotropic consolidation curves for Toyoura sand samples prepared using three different methods (Ishihara, 1993)

LIQUEFACTION VULNERABILITY

A lack of a suitable parameter exists at present to classify any given soil according to its intrinsic vulnerability against liquefaction. Some general ideas have been presented in this regard, and they have basically been established based on the shape of the grain size distribution curves (Tsuchida, 1970; Ishihara et al., 1980). It is well known however that there are others factors that also control the liquefaction vulnerability of a cohesionless soil, for example, particle shape, particle hardness, fines content (Verdugo, 1989), and plasticity of the fines. All of these factors that are not dependent on the state of a soil mass, and are material properties, are somewhat reflected in the location of the steady state line and on the position of both the consolidation curves of the loosest and densest state. In order to define a parameter that reflect to some extent the intrinsic potential of liquefaction of a given material, therefore these three references curves will be considered.

In a cohesionless material, the projection of the steady state line in the *e-p'* plane represents the combination of void ratio, and effective mean stress attained ultimately when the soil is deformed greatly. For a homogeneous soil mass, the steady state line is a unique reference line unaffected by the type of soil deposition and initial state conditions of density and pressure. It is also independent of whether the load is drained or undrained. For an undrained loading condition, the steady state line provides a very stable and physically meaningful reference line dividing those states that ultimately develop either positive or negative pore pressure. Although it may be thought that the quasi steady state line can also be used as a reference line, this idea does not work when an intrinsic soil property is expected to be defined. This restriction comes from the fact that the quasi steady state line is strongly affected by the initial soil fabric (Verdugo, 1992; Ishihara, 1993).

The isotropic consolidation curves for the loosest and densest states provide a set of boundaries for any possible soil state. If attention is drawn to the position of the steady state line with respect to these two boundaries, it is possible to realize that when the steady state line is located very close to the upper boundary defined by the isotropic consolidation line of the loosest state, as shown in Fig. 14(a), the area, A_c, that is associated with those states where the soil mass can be potentially unstable is small. Conversely, Fig. 14(b) shows a material with a steady state line closer to the isotropic consolidated curve of the densest state, hence with a dilative area, A_d, rather small. In this situation, there exists a significant possibility for the soil deposit to be in such states that can develop a contractive response associated to a flow failure or "true liquefaction". Consequently, it is suggested that according to the relative position of these curves with respect to each other, it is possible to evaluate the intrinsic vulnerability of a given soil against liquefaction. Thus a parameter of the form of $A_c/(A_c+A_d)$ seems to be an appropriate parameter concerned the intrinsic liquefac-

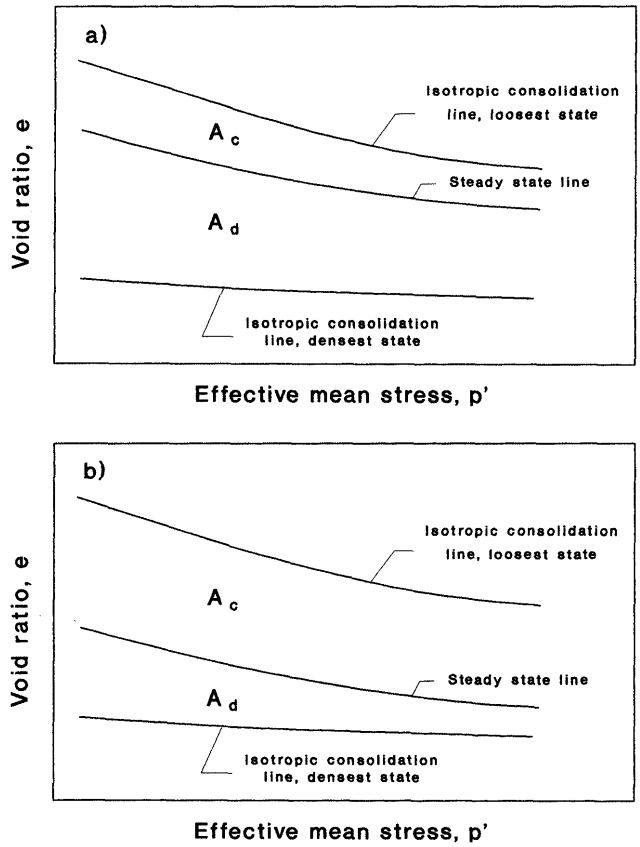

Fig. 14. Representation of a soil with a) small vulnerability against liquefaction; b) large vulnerability against liquefaction

tion potential. Figure 15 illustrates the areas A_c and A_d considering the general trend of the steady state line and the isotropic consolidation lines for the loosest and densest states. It is important to note, that for high pressure the loosest and densest states merge with each other which has been shown experimentally by Vesic et al. (1968) and Miura et al. (1984), among others. In addition, it is well known that under a sufficiently high pressure, the soil behavior is fully contractive independent of the initial void ratio. This means that in the e-p' plane the steady state line, for high pressures, must be located to the left and below the isotropic consolidation lines. It is clear, however, that for a low pressure and an initial dense state, the soil behavior is dilative which implies that the steady state line has to be located to the right of the isotropic line for the densest state. Therefore, in the e-log p plane, the steady state line has to cross the isotropic consolidation line for the densest state.

From a practical point of view, the complete evaluation of the areas A_c and A_d is difficult, because it would be necessary to use very high pressure in order to evaluate the consolidation curves to the point where they merge with each other. It seems reasonable nevertheless, to make a simplification and only take into account the ratio between the range of void ratios where the soil is contractive and the total range of void ratios where the soil can exist for an arbitrary value of effective mean stress of 0.1 MPa. In order to account for the intrinsic potential of liquefaction of a given soil, the index property, Relative Contractiveness, R_c, is proposed which is expressed as follows,

$$R_c=\frac{(e_{\max})_1-(e_{ss})_1}{(e_{\max})_1-(e_{\min})_1} \tag{2}$$

Figure 16 shows schematically $(e_{\max})_1$, $(e_{\min})_1$ and $(e_{ss})_1$ which denote respectively, the maximum, minimum and steady state void ratios, all for an effective mean stress of 0.1 MPa. If the proposed approximation of the isotropic line for the densest state is used, the value of $(e_{\min})_1$ would be equal to $e_{\min}$. It should be noted that the defined relative contractiveness, R_c, is not a parameter specifying a state of the soil, but is rather an index representing an intrinsic material property which is largely dependent on the grain composition of a soil. It is important also to keep in mind that the actual resistance against liquefaction is a function of the state of the material. From a theoretical point of view, R_c may have values between 0 and 1. A value of $R_c=1$ represents a hypothetical soil that for any initial states will have a contractive response, whereas $R_c=0$ represents a hypothetical soil that will always have a dilative response. For real soils, R_c should have a tendency to be closer to 0 or 1 according to the intrinsic capacity of contraction or dilatation of the soil. For Toyoura

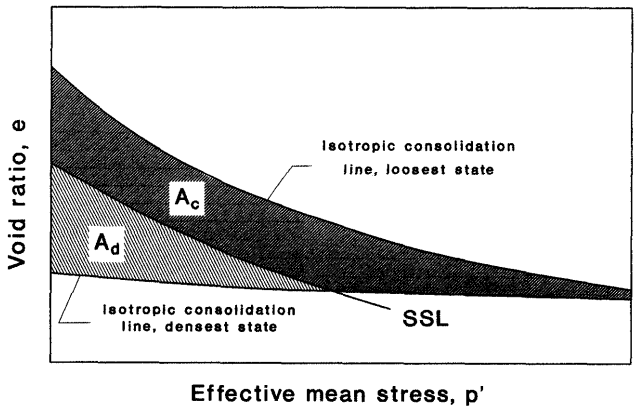

Fig. 15. State diagram indicating the contractive and dilative regions

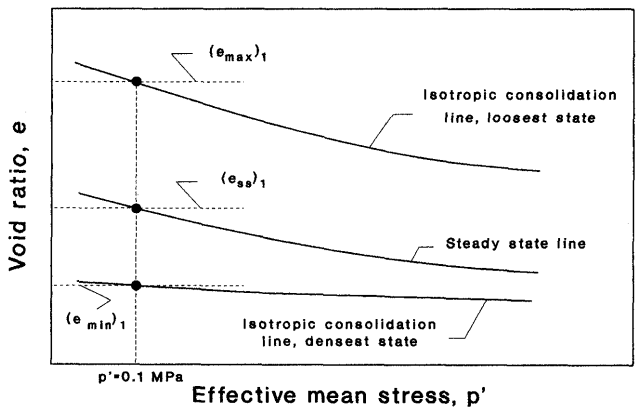

Fig. 16. Definition of the relative contractiveness, R_c

sand, Fig. 17 shows the location of the loosest and densest isotropic consolidation curves and the steady state line. It is important to note that the loosest state achieved by the moist placement sample preparation method reproduces a state looser than the one obtained by the conventional procedure using dry soil. In addition, in Fig. 17 for 0.1 MPa, the corresponding values of $(e_{max})_1$, $(e_{min})_1$ and $(e_{ss})_1$ are shown. For this sand the relative contractiveness has a value, $R_c=0.25$, which can be considered as a fairly small contractive material.

Different sandy soils containing low plastic fines and silty soils classified as ML were tested following the same procedure explained above; the corresponding relative contractiveness, R_c, was evaluated and plotted against the fines content in Fig. 18. The set of data for each soil is presented elsewhere (Verdugo, 1992). The soil with 100% fines was produced from the Toyoura sand crushing it by means of a ball-mill. As can be seen in Fig. 18, the value of R_c tends to increase with increasing fines content leading to the conclusion that the more low plastic fines content, the greater would be the opportunity for the soil to exist in the field in a contractive state that can induce flow failure or liquefaction.

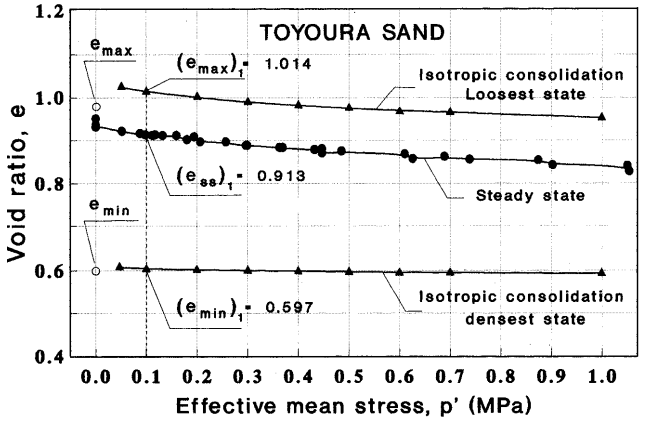

Fig. 17. Steady state line and the isotropic consolidation curves for the loosest and densest state of Toyoura sand

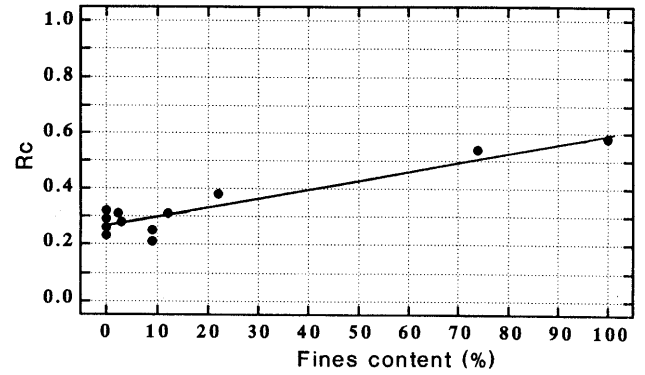

Fig. 18. Effect of the low plastic fines content on the relative contractiveness

CONCLUSIONS

It has been shown that in those cases of undrained loading with peak strength, there exist two conditions that may be associated with the steady state of deformation. The first one corresponds to the development of the minimum strength, and it has been named the quasi steady state. It is developed at a small to medium level of deformation, typically between 1 to 16% of axial strain. The second condition is achieved at a high level of deformation, typically beyond 25% of axial deformation, and it is associated with the ultimate state developed by the soil sample. This ultimate condition corresponds to the actual steady state, and it is always achieved irrespective of the initial state of the soil sample and whether the response is contractive or dilative. Conversely, the quasi steady state can only occur when the initial states of the soil are well above the steady state line, so the response is contractive.

The experimental results strongly indicated that the steady state or ultimate condition is not affected by the initial confining pressure. The results have shown, however, that the quasi steady state is slightly affected by the initial confining pressure, but for practical purposes it seems reasonable to assume that it is independent.

A series of undrained tests conducted under different initial effective confining pressures, but at the same void ratio after consolidation, have indicated identical effective stress paths during unloading from the steady state condition. This observation strongly supports the idea of Casagrande regarding the existence of a unique fabric developed during the steady state.

The results of drained tests at large deformations indicate the existence of an ultimate state without volumetric strain and continuous deformation under constant shear stress. The ultimate states evaluated from drained tests are in good agreement with the steady state obtained from undrained tests. At large deformations, therefore, both undrained and drained loading conditions converge to the same curve in the *e-q-p'* space, which corresponds to the steady state line.

Based on the range of void ratios where the soil response is contractive with respect to the total range of void ratio where a soil can exist for an effective mean stress of 0.1 MPa, the parameter, Relative Contractiveness, R_c, is proposed to evaluate the intrinsic potential of liquefaction for a given soil. The larger the value of R_c the larger the intrinsic potential of liquefaction for a given soil.

ACKNOWLEDGMENTS

The authors gratefully acknowledge the financial support provided by the Ministry of Education, Science and Culture, Government of Japan (MONBUSHO) which made this present study possible.

REFERENCES

1) Alarcon-Guzman, A., Leonards, G. and Chameau, J. (1988): "Undrained monotonic and cyclic strength of sands," Journal of Geotechnical Engineering, ASCE, Vol. 114, No. 10, pp. 1089–1109.
2) Been, K. and Jefferies, M. G. (1985): "A state parameter for sands," Géotechnique, Vol. 35, No. 2, pp. 99–112.
3) Been, K., Jefferies, M. G. and Hachey, J. (1991): "A critical state of sands," Géotechnique, Vol. 41, No. 3, pp. 365–381.
4) Casagrande, A. (1936): "Characteristics of cohesionless soils affecting the stability of slopes and earth fills," Journal of the Boston Society of Civil Engineering, January, pp. 13–32.
5) Casagrande, A. (1975): "Liquefaction and cyclic deformation of sands—a critical review," Fifth Panamerican Conference on Soil Mechanics and Foundation Engineering, Buenos Aires, Argentina.
6) Castro, G. (1969): "Liquefaction of sands," Harvard Soil Mechanics Series, No. 81, Cambridge, Mass.
7) Castro, G. (1975): "Liquefaction and cyclic mobility of saturated sands," Journal of Geotechnical Engineering, ASCE, Vol. 101, No. GT6, June, pp. 551–569.
8) Castro, G., Poulos, S., France, J. and Enos, J. (1982): "Liquefaction induced by cyclic loading," Geotechnical Engineering, Inc., Reporter Submitted to National Science Foundation, March.
9) Dobry, R., Vasquez-Herrera, A., Mohamad, R. and Vucetic, M. (1985): "Liquefaction flow failure of silty sand by torsional cyclic tests," Advances in the Art of Testing Soils Under Cyclic Conditions, ASCE, Khosla, Vija (ed.).
10) Ishihara, K. (1993): "Liquefaction and flow failure during earthquakes," The 33rd Rankine Lecture, Géotechnique, Vol. 43, No. 3, pp. 351–415.
11) Ishihara, K., Tatsuoka, F. and Yasuda, S. (1975): "Undrained deformation and liquefaction of sand under cyclic stresses," Soils and Foundation, Vol. 15, No. 1, pp. 29–44.
12) Ishihara, K., Troncoso, J. H., Kawase, Y. and Takahashi, Y. (1980): "Cyclic strength characteristics of tailing material," Soils and Foundations, Vol. 20, No. 4, pp. 128–142.
13) Ishihara, K., Verdugo, R. and Acacio, A. A. (1991): "Characterization of cyclic behavior of sand and post-seismic stability analyses," Proceedings of the 9th Asian Regional Conference on Soil Mechanics and Foundation Engineering, Bangkok.
14) Miura, N., Murata, H. and Yasufuku, N. (1984): "Stress-strain characteristics of sand in a particle-crushing region," Soils and Foundations, Vol. 24, No. 1, pp. 77–89.
15) Negussey, D., Wijewickreme, K. and Vaid, Y. (1988): "Constant-volume friction angle of granular materials," Canadian Geotechnical Journal, Vol. 25, pp. 50–55.
16) Oda, M., Koishikawa, I. and Higuchi, T. (1978): "Experimental study of anisotropic shear strength of sand by plane strain test," Soils and Foundations, Vol. 18, No. 1, pp. 25–38.
17) Poulos, S. J. (1981): "The steady state of deformation," Journal of Geotechnical Engineering Division, ASCE, Vol. 107, No. GT5, May, pp. 553–562.
18) Poulos, S. J., Castro, G. and France, J. W. (1985): "Liquefaction evaluation procedure," Journal of Geotechnical Engineering, ASCE, Vol. 111, No. 6, pp. 772–791.
19) Roscoe, K. H., Schofield, A. N. and Wroth, C. P. (1958): "On yielding of soils," Géotechnique, Vol. 8, No. 1, pp. 22–53.
20) Sladen, J. A., Handford, G. (1987): "A potential systematic error in laboratory testing of very loose sands," Canadian Geotechnical Journal, Vol. 24, pp. 462–466.
21) Tsuchida, H. (1970): "Prediction and countermeasure against the liquefaction in sand deposits," Abstract of the Seminar in the Port and Harbor Research Institute, pp. 3.1–3.33 (in Japanese).
22) Verdugo, R. (1989): "Effect of fines content on the steady-state of deformation on sandy soils," Master Thesis, Department of Civil Engineering, University of Tokyo, Japan.
23) Verdugo, R. (1992): "Characterization of sandy soil behavior under large deformation," Doctoral Thesis, Department of Civil Engineering, University of Tokyo, Japan.
24) Vesic, A. and Clough, W. (1968): "Behavior of granular materials under high stresses," Soil Mechanics and Foundation Engineering Division, ASCE, Vol. 94, No. SM3, pp. 661–668.